2007 IEEE International Conference on
Robotics and Automation
Roma, Italy, 10-14 April 2007

Using time-reversal symmetry for stabilizing a simple 3D walker model

Gijs van Oort
Dept. of Electrical Engineering
University of Twente, The Netherlands
Email: g.vanoort@ewi.utwente.nl

Stefano Stramigioli
Dept. of Electrical Engineering
University of Twente, The Netherlands
Email: s.stramigioli@ieee.org

***Abstract*— A new method is presented for controlling the lateral foot placement of a simple 3D compass biped model. The method is based on the fact that, in the limit cycle, the gait is time-reversal symmetric and that, after a disturbance, the degree of asymmetry is indicated by a single variable. This variable is used for feedback with a proportional controller. Simulation results show that the controller works very well for a large range of gaits, without any adaptation of the parameter values.**

I. Introduction

Dynamically walking robots, in simulation (e.g. [1], [2]), as well as in practice (e.g. Denise [3], Dribbel [4] and the Cornell Walker [5]), have the advantage over 'fully actuated' walkers that they consume far less energy. However, stability and robustness are serious problems for them. Particularly, the robustness of 3D dynamic walkers to lateral disturbances is still very poor. Lateral foot placement is generally seen as a promising method for increasing the robustness in the sideways direction.

This article presents a new method for controlling the lateral foot placement of a simple 3D compass biped model. It is based on the fact that, in the limit cycle, the gait is time-reversal symmetric and that, after a disturbance, the degree of asymmetry is indicated by a single variable. This variable is used for feedback with a proportional controller.

In section II the model of the 3D compass walker is presented. The configuration of the walker is given, the environmental assumptions are summed up and the equations of motion as well as the impact equations are discussed. In section III the open-loop gait is analyzed. It is shown that the system has infinitely many limit cycles. One 'reference limit cycle' is chosen and by linearization it is shown that the limit cycle is unstable. It is also shown that a few eigenvalues are intrinsic to the model and cannot be changed. In section IV we show that each step is time-reversal symmetric when the walker is in its limit cycle. In section V we use this knowledge and propose a controller with one parameter K, and in section VI we show by simulation that the controller can stabilize the walker well for a large range of gaits. We give a different view of the controller in section VII and we end with conclusions and recommendations in section VIII.

II. Model description

A. General

Consider a 3D compass biped model as sketched in figure 1. This biped consists of a pointmass at the hip, having mass m, and two massless legs of length ℓ; each with two degrees of freedom: φ_{hip} and φ_{splay} (the hip can thus be seen as a ball-joint). We distinguish the stance leg (subscripted st) and the swing leg (subscripted sw). The 'feet' are modeled as point contacts. Ground contact is inelastic and rigid, and since the legs are infinitely stiff, the support transfer is instantaneous. The ground is considered to have an infinite friction coefficient: no sliding of the feet can occur. In this article the following parameters were chosen: m=1 kg; ℓ=1 m; g=+9.81 m/s^2 (gravitational acceleration).

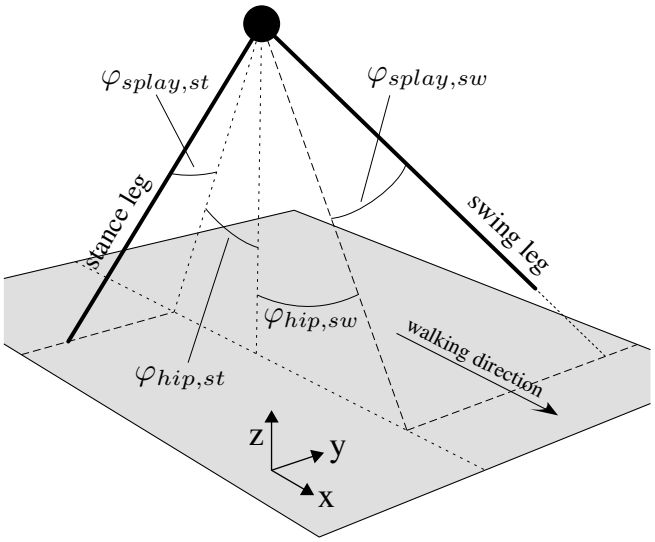

Fig. 1. A sketch of the 'very simple 3D biped' used in this article. Walking direction is the positive x-direction.

The state of the system represents the position and velocity of the hip, relatively to the stance foot, and is denoted as follows: $\mathbf{x} = (\varphi_{hip,st}, \dot{\varphi}_{hip,st}, \varphi_{splay,st}, \dot{\varphi}_{splay,st})^T$. The state at the beginning of a step k, which is just after swing foot impact, when the rear foot leaves the ground, is denoted by $\mathbf{x}_k^+$ (the $+$ indicates 'post-impact'). The state at the end of the step, just before the new foot impact, is denoted by $\mathbf{x}_k^-$ (the $-$ indicates 'pre-impact'). Note that the state $\mathbf{x}_k^+$ occurs well before $\mathbf{x}_k^-$ and that $\mathbf{x}_k^-$ is immediately followed by $\mathbf{x}_{k+1}^+$ after the impact.

The only means of control of this model is giving the next pose for the swing leg. Because the legs are considered massless, the new configuration can be considered to be reached instantaneously and without any dynamic influence

$$p_{add} = m\ell \, \frac{\sin \mathbf{u}_2 \left(\dot{\varphi}^-_{splay} \, \cos \varphi^-_{splay} \right) + \cos \mathbf{u}_2 \left(\dot{\varphi}^-_{splay} \, \sin \varphi^-_{splay} \, \cos(\varphi^-_{hip} - \mathbf{u}_1) + \dot{\varphi}^-_{hip} \, \cos \varphi^-_{splay} \, \sin(\varphi^-_{hip} - \mathbf{u}_1) \right)}{1 - \sin \mathbf{u}_2 \, \sin \varphi^-_{splay} + \cos \mathbf{u}_2 \, \cos \varphi^-_{splay} \, \cos(\varphi^-_{hip} - \mathbf{u}_1)} \tag{2}$$

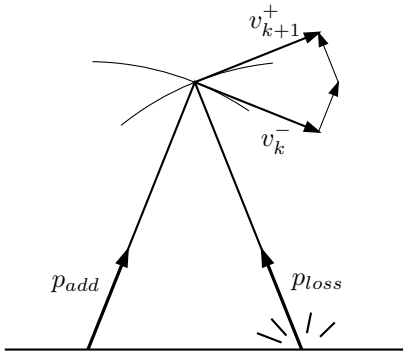

Fig. 2. A 2D representation of the impulses during foot impact.

on the overall motion. The input of the system is defined as $\mathbf{u} = (\varphi_{hip,sw}, \varphi_{splay,sw})^T$. The input at the end of step k, before and during impact, is denoted by $\mathbf{u}_k$.

B. Equations of motion

During a step, the hip mass plus leg acts as a spherical inverted pendulum, pivoting around the stance foot. The corresponding equations of motion are:

$$\begin{cases} \ddot{\varphi}_{hip} \;\; = \dfrac{\frac{g}{\ell} \sin(\varphi_{hip}) + 2\, \dot{\varphi}_{hip}\, \dot{\varphi}_{splay} \sin(\varphi_{splay})}{\cos(\varphi_{splay})} \\ \ddot{\varphi}_{splay} = \frac{g}{\ell} \cos(\varphi_{hip}) \sin(\varphi_{sp}) - \dot{\varphi}^2_{hip} \cos(\varphi_{sp}) \sin(\varphi_{sp}) \end{cases} \tag{1}$$

where all angles $\varphi_\bullet$ refer to the stance leg. These equations can be integrated to obtain the state of the system. Because the swing leg is massless, it does not influence the motion of the system during the step. Therefore, the input $\mathbf{u}$ does not appear in the equations.

C. Impact equations and energy injection

When the swing foot hits the ground (foot impact), energy is lost and velocity of the hip changes instantaneously. The inelastic, instantaneous collision is modeled as the ground applying an upward impulse p_{loss} to the walker, along the leg. The loss of kinetic energy due to this impulse is denoted by E_{loss}. In order to keep the internal energy of the walker at level, energy is added to the system by applying an upward impulse p_{add} along the posterior leg (which becomes the new swing leg). This impulse can be interpreted as the equivalent of the push-off of the human ankle during a normal gait. The kinetic energy added to the system is denoted by E_{add}. In order to keep the energy level constant, we need to find a p_{add} such that $E_{add} = E_{loss}$. Since we consider the push-off with energy injection right before the swinging leg touches the floor, p_{loss} is dependent on p_{add}. To understand this, it is sufficient to consider the extreme case in which p_{add} would be extremely large. In this situation the walker would be launched and the front leg would not even touch the ground.

Given the state of the walker $(\mathbf{x}^-_k, \mathbf{u}_k)$ just before impact, the required impulse p_{add} can be calculated that makes $E_{loss} = E_{add}$ using (2) which is given without proof. In (2) all $\varphi^-_\bullet$'s refer to the (pre-impact) stance leg. Note that the energy injection system is actually identical to the energy loss system: it is an impulse along the leg that adds a certain amount of velocity to the walker, in the direction of the leg. If time would be reversed (which makes the walker walk backward), the impulses take each others place, and the system would still walk. In other words: the impact (including energy injection) is time-reversal symmetric.

We can define the impact equations (including the energy injection) as a nonlinear function in the following way: $\mathbf{x}^+_{k+1} = \mathcal{I}(\mathbf{x}^-_k, \mathbf{u}_k)$. The input $\mathbf{u}_k$ defines the position of pre-impact swing leg, which becomes the post-impact stance leg. The position of this stance leg can directly be copied from $\mathbf{u}_k$ to two of the elements of $\mathbf{x}^+_{k+1}$. From this it follows that $\mathbf{x}^+_{k+1}$ always has the form:

$$\mathbf{x}^+_{k+1} = \begin{pmatrix} \varphi^+_{hip} \\ \dot{\varphi}^+_{hip} \\ \varphi^+_{splay} \\ \dot{\varphi}^+_{splay} \end{pmatrix} = \mathcal{I}(\mathbf{x}^-_k, \mathbf{u}_k) = \begin{pmatrix} \mathbf{u}_{k,1} \\ \mathcal{I}_2(\mathbf{x}^-_k, \mathbf{u}_k) \\ \mathbf{u}_{k,2} \\ \mathcal{I}_4(\mathbf{x}^-_k, \mathbf{u}_k) \end{pmatrix} \tag{3}$$

where the second and fourth element are non-linear functions of the input variables, and the first and third element are equal to the input itself. The equations are quite long and not included in this article. They can however be found in [6].

D. Stride function

We define the *stride function*:

$$\mathbf{x}^+_{k+1} = \mathcal{S}(\mathbf{x}^+_k, \mathbf{u}_k) \tag{4}$$

which, given a certain initial state $(\mathbf{x}^+_k, \mathbf{u}_k)$ returns the state $\mathbf{x}^+_{k+1}$ at the beginning of the next step (if it exists). The stride function covers the equations of motion (subsection II-B) as well as the impact equations and energy injection system (subsection II-C). Similarly to (3), it can be found that the stride function has the form:

$$\mathbf{x}^+_{k+1} = \begin{pmatrix} \varphi^+_{hip} \\ \dot{\varphi}^+_{hip} \\ \varphi^+_{splay} \\ \dot{\varphi}^+_{splay} \end{pmatrix} = \mathcal{S}(\mathbf{x}^+_k, \mathbf{u}_k) = \begin{pmatrix} \mathbf{u}_{k,1} \\ \mathcal{S}_2(\mathbf{x}^+_k, \mathbf{u}_k) \\ \mathbf{u}_{k,2} \\ \mathcal{S}_4(\mathbf{x}^+_k, \mathbf{u}_k) \end{pmatrix}. \tag{5}$$

It should be noted that, apart from disturbances, the internal energy of the system is always constant ($\dot{H} = 0$, where $H = E_{kin} + E_{pot}$). During the motion phase, the system moves through a conservative (gravity) field, which of course does not alter the total internal energy. During

TABLE I

THE EIGENVALUES AND EIGENVECTORS OF THE UNCONTROLLED WALKER, LINEARIZED AROUND THE 'REFERENCE GAIT'.

eigenvalue	-2.26	1	0	0
eigenvector	$\begin{pmatrix} 0 \\ -0.05 \\ 0 \\ -0.99 \end{pmatrix}$	$\begin{pmatrix} 0 \\ -0.99 \\ 0 \\ -0.08 \end{pmatrix}$	$\begin{pmatrix} 0 \\ 0.10 \\ 0.37 \\ -0.92 \end{pmatrix}$	$\begin{pmatrix} 0.46 \\ -0.89 \\ 0 \\ 0.05 \end{pmatrix}$

impact, the amount of (kinetic) energy added by p_{add} is (by construction) exactly equal to the amount that is lost by p_{loss}. So, if a disturbance would raise (or lower) the total internal energy of the walker, the system has no way to restore the energy to the original level afterwards.

III. ANALYSIS OF THE UNCONTROLLED GAIT

For any fixed $\mathbf{u}$ within the range where the walker looks 'human-like', thus with the hip above the ground, swing leg pointing forward and step length larger than step width, this system has infinitely many limit cycles $\mathbf{x}_{k+1}^+ = \mathbf{x}_k^+$, which will be denoted by $\mathbf{x}^*$.

To understand this, realize that this model has its energy addition directly coupled to the energy loss. For each energy level the loss and addition are in equilibrium, which gives the possibility for a limit cycle for each energy level. This is different from most other walker models, that inject a fixed amount of energy into the system at each step, and can have a limit cycle only for a gait where the impact energy loss is equal to this fixed amount of injected energy. For our walker, it can be seen that all limit cycles for a given $\mathbf{u}$ lie on a (one-dimensional) curve in the state space. This will be proven in the appendix.

For analysis it is convenient to choose a 'reference gait'. Quite arbitrarily a limit cycle is chosen having $\mathbf{u}^r = (-0.3, 0.05)^T$ and $\mathbf{x}^r = (-0.3, 1.5, 0.05, -0.0819)^T$. By linearizing the stride function $\mathcal{S}$ around $(\mathbf{x}^r, \mathbf{u}^r)$ and taking the eigenvalues of the obtained Jacobian matrix $J_x = \frac{\partial \mathcal{S}}{\partial x}$, it can be shown that this gait is unstable. The other limit cycle gaits in the 'human-like' range are also unstable. The eigenvalues and corresponding eigenvectors of the reference gait are shown in table I. The eigenvalues are discussed below.

From (5) it can be seen that the first and third element of $\mathcal{S}$ are independent on $\mathbf{x}$, hence the first and third row of J_x will be entirely zero. J_x thus has rank 2 (the two other rows are linearly independent), so it can only have two non-zero eigenvalues (the other two will be zero).

If a disturbance would alter the magnitude of the velocity of the walker, the kinetic energy and thus the total energy H will also change (by, say, an amount of ΔH). By construction, the walker cannot restore its original energy level, so the deviation from the original energy level will always remain constant (equal to ΔH), which explains the eigenvalue 1.

The eigenvalue of -2.26 has to do with changes in direction of the velocity vector. This is inverted pendulum-like, unstable mode that needs to be stabilized by means of active control.

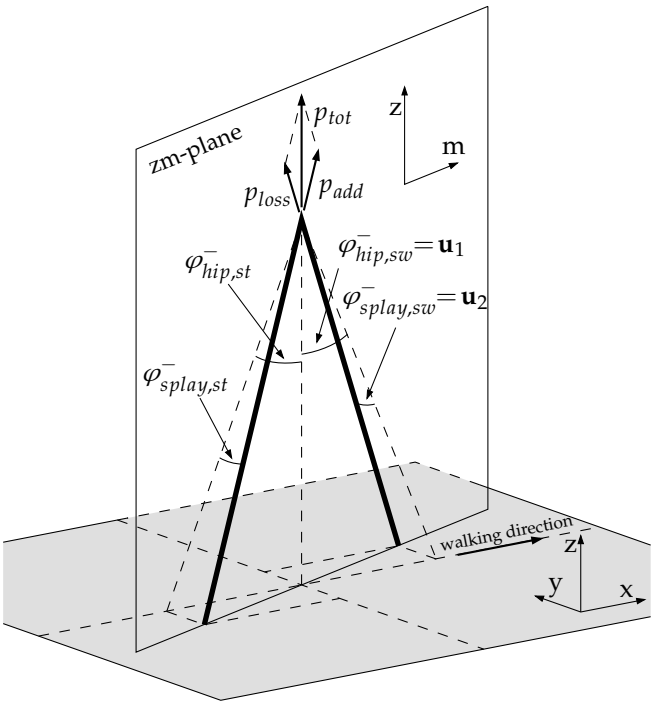

Fig. 3. A special case for the impact equations: $\varphi^-_{hip,st} = -\mathbf{u}_1$, $\varphi^-_{splay,st} = \mathbf{u}_2$. In this case the legs span a plane that is exactly vertical.

If the walker falls, we can distinguish the following cases:

- The walker is falling backward ($\dot{\varphi}_{hip} < 0$). This happens when not enough energy is present at the start of a step. As an indication, if for our reference input $\mathbf{u}^r$ the initial hip velocity $a = \dot{\varphi}_{hip} < 0.94$ rad/s, the walker will fall backwards.
- The walker is falling to the side. This happens if the splay velocity or the splay angle is too far off the limit cycle value.
- The walker goes so fast that the stance foot leaves the ground due to the vertical component of the ground reaction force becoming zero. This happens when the angular velocity of the hip (rotating around the stance foot) is so large that $m\ell\omega^2(\cos\varphi_{hip}\cos\varphi_{splay}) > mg$. As an indication, if for our reference input $\mathbf{u}^r$ the initial hip velocity $a = \dot{\varphi}_{hip} > 3.15$ rad/s, the walker will leave the ground. The walker cannot fall forwards, because it always instantaneously puts its swing leg forward.

IV. USING TIME-REVERSAL SYMMETRY FOR THE DESIGN OF A CONTROLLER

A special case for the impact equations (3) occurs when the position of the stance leg just before impact is equal but mirrored to the (fixed) input, which is the position of the

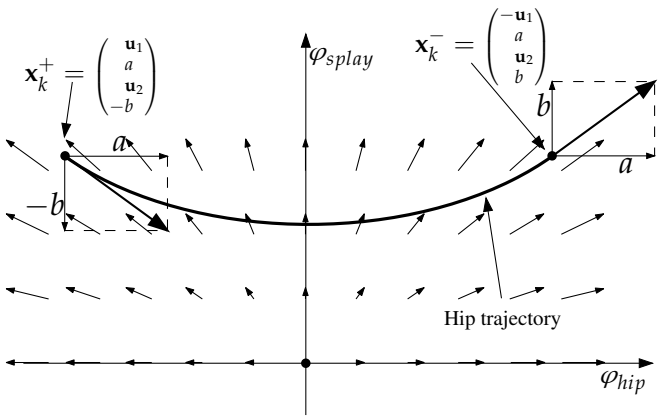

Fig. 4. The trajectory traveled by the hip when going from the initial condition $\mathbf{x}_k^+$ to the final condition $\mathbf{x}_k^-$, along with an approximation of the (angular) acceleration vector field of (1). Because the conditions and the vector field are symmetric around $\varphi_{hip} = 0$, the trajectory is also symmetric.

swing leg:

$$\mathbf{x}^- = \begin{pmatrix} \varphi_{hip,st}^- \\ \dot{\varphi}_{hip,st}^- \\ \varphi_{splay,st}^- \\ \dot{\varphi}_{splay,st}^- \end{pmatrix} = \begin{pmatrix} -\mathbf{u}_1 \\ a \\ \mathbf{u}_2 \\ b \end{pmatrix} = \begin{pmatrix} -\varphi_{hip,sw} \\ a \\ \varphi_{splay,sw} \\ b \end{pmatrix} \tag{6}$$

with any positive angular velocities a and b. In this case, the plane spanned by the legs, indicated as the zm-plane in figure 3, will be exactly vertical (the z-axis will be parallel to the world's z-axis and the m-axis will be parallel to the world's xy-plane. Because the two impact impulses p_{add} and p_{loss} are aligned with the legs, they also lie in the zm-plane. Both impulses are equal in magnitude, so their z-components add up, while their m-components cancel each other out. So only the vertical velocity of the hip will change at impact; the forward and sideways velocities are unaffected. This makes the post-impact velocities be equal but mirrored (due to the splay sign change) to the pre-impact velocities, resulting in the following post-impact state:

$$\text{Equation (6)} \Longrightarrow \mathbf{x}^+ = \begin{pmatrix} \varphi_{hip}^+ \\ \dot{\varphi}_{hip}^+ \\ \varphi_{splay}^+ \\ \dot{\varphi}_{splay}^+ \end{pmatrix} = \begin{pmatrix} \mathbf{u}_1 \\ a \\ \mathbf{u}_2 \\ -b \end{pmatrix} \tag{7}$$

which holds for any angular velocities a and b. If we can find values for a and b such that the equations of motion, when initialized with post-impact state $\mathbf{x}^+$, as defined in (7), will return a new pre-impact state $\mathbf{x}^-$ obeying (6), we obtain a limit cycle as schematically reported below:

$$\mathbf{x}_k^+ = \begin{pmatrix} \mathbf{u}_1 \\ a \\ \mathbf{u}_2 \\ -b \end{pmatrix} \overset{(1)}{\Longrightarrow} \mathbf{x}_k^- = \begin{pmatrix} -\mathbf{u}_1 \\ a \\ \mathbf{u}_2 \\ b \end{pmatrix} \overset{(3)}{\Longrightarrow} \mathbf{x}_{k+1}^+ = \begin{pmatrix} \mathbf{u}_1 \\ a \\ \mathbf{u}_2 \\ -b \end{pmatrix} \overset{(1)}{\Longrightarrow} \dots \tag{8}$$

In figure 4 the trajectory (the solution of the differential equation (1) with the given initial conditions $\mathbf{x}_k^+$ and final conditions $\mathbf{x}_k^-$) is sketched, along with an approximation of the acceleration vector field of (1).[1] Because the initial and final conditions as well as the vector field are symmetric around $\varphi_{hip} = 0$, the trajectory will also be symmetric. This symmetry implies that the sideways velocity $\dot{\varphi}_{splay}$ at $\varphi_{hip} = 0$ must be zero. At the same time, because the vector field is symmetric around $\varphi_{hip} = 0$, any trajectory having $\dot{\varphi}_{splay}|_{(\varphi_{hip}=0)} = 0$ will be symmetric around $\varphi_{hip} = 0$, and —combined with the impact equations— will give a limit cycle. So, for this walker, the condition $\dot{\varphi}_{splay}|_{(\varphi_{hip}=0)} = 0$ is a sufficient condition for having a limit cycle. We introduce $\mathcal{Y}$ as a shorter notation:

$$\mathcal{Y} := \dot{\varphi}_{splay}|_{(\varphi_{hip}=0)} . \tag{9}$$

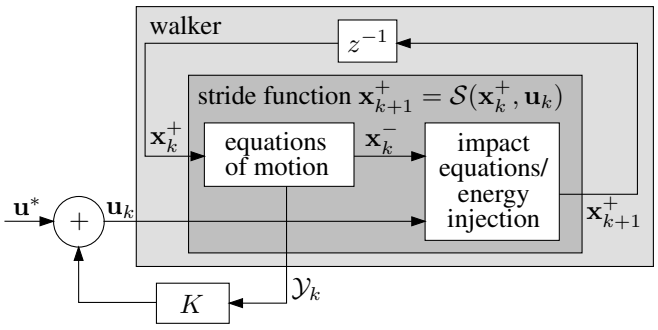

Fig. 5. A block diagram of the controlled walker.

V. Control

If the walker is walking in a limit cycle ($\mathcal{Y} = 0$), a disturbance will generally lead to a non-zero $\mathcal{Y}$. We can use the value of $\mathcal{Y}$ at step k (denoted as $\mathcal{Y}_k$) to control the input $\mathbf{u}_k$, such that the disturbance is suppressed (i.e. $|\mathcal{Y}_{k+1}| < |\mathcal{Y}_k|$). Note that $\mathbf{u}_k$ is only used at the end of step k and that $\mathcal{Y}_k$ is already known halfway step k, so we won't run into problems here. A good choice for control would be to give a setpoint offset for the splay angle $\varphi_{splay,sw}$ proportional to $\mathcal{Y}$:

$$\mathbf{u}_k = \begin{pmatrix} \varphi_{hip,sw} \\ \varphi_{splay,sw} \end{pmatrix} = \begin{pmatrix} \mathbf{u}_1^* \\ \mathbf{u}_2^* + K \cdot \mathcal{Y}_k \end{pmatrix}$$

where K is the controller gain. A block diagram of the obtained system is shown in figure 5. Analysis of the effect of a disturbance, sketched in figure 6, shows that K should be positive. Because of the extensiveness of the equations of motion and the impact equations, no attempt was made to analytically prove that the walker can indeed be stabilized with this control law. However, simulation results, described in the next section, have shown that it is indeed possible to stabilize the walker.

An advantage of the controller over the conventional technique of linearization and pole placement (e.g. [1]) is that no explicit knowledge of the limit cycle is needed in order to stabilize the walker (as $\mathbf{x}^*$ does not appear in the

[1]The actual acceleration at a certain point also depends on the instantaneous velocity of the hip. However, for the velocities used, the influence is small.

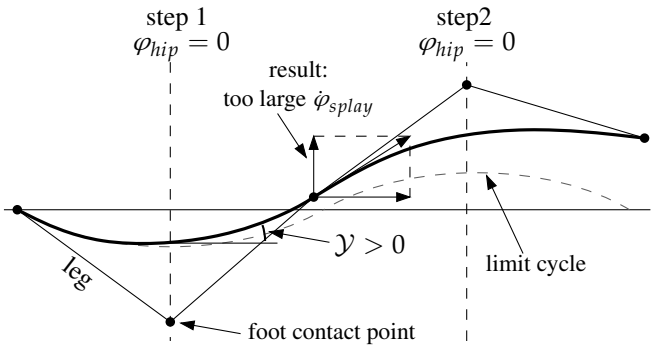

Fig. 6. Analysis of the effect of a disturbance. A disturbance causing $\mathcal{Y}$ to be positive (as in the figure), leads to a too large $\dot{\varphi}_{splay}$. In order to compensate for this, the swing foot should be placed a little more outward.

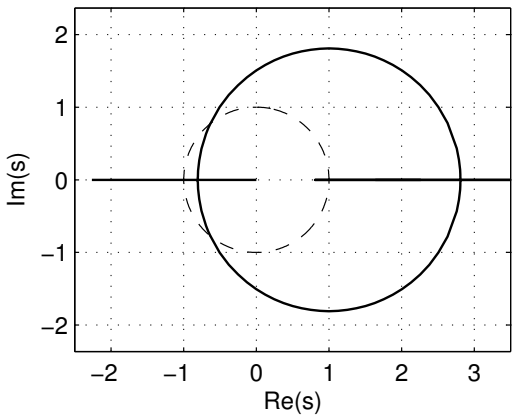

Fig. 7. Root locus plot of the controlled reference gait. For $K = 0.252 \ldots 0.398$ all poles are within the unit circle, so the system is stable. The smallest eigenvalue is reached at $K = 0.259$.

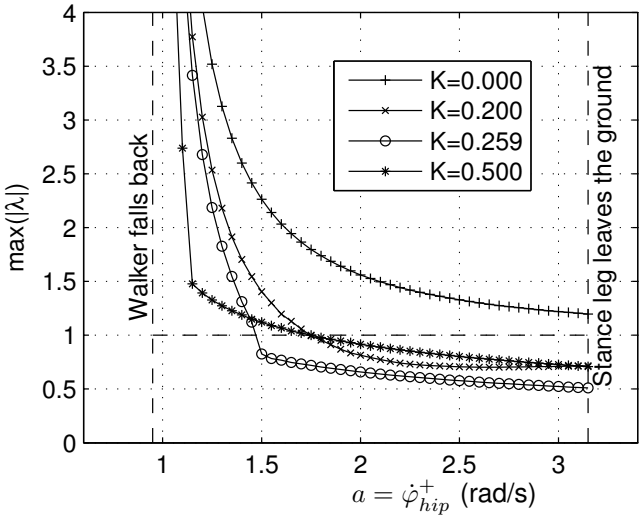

Fig. 8. The eigenvalues of the controlled system for different gait velocities, with different values for K. It can be seen that $K = 0.259$ can not only stabilize our reference gait well, but also all gaits with higher velocity.

calculation of $\mathbf{u}_k$). Hence, the controller will work for a great range of limit cycles without adaptation of any parameter. Furthermore, only a single controller gain needs to be chosen, which simplifies the design and tuning.

VI. Simulation results

In order to verify the correctness of the control strategy, simulations were done in Matlab. The results are presented in this section.

One criterion that could be used for choosing the 'optimal' value of K is trying to minimize the eigenvalues of the linearized controlled system. For a non-zero K, the third element of the stride function S will become dependent on $\mathbf{x}_k^+$ (because $\mathbf{u}_{k,2}$ is dependent on $\mathbf{x}_k^+$), so the third row of the Jacobian J_x will not be zero anymore. This results in an increase in rank of J_x and the possibility to have three non-zero eigenvalues. One of them is the (unchangeable) eigenvalue 1, which is still a system property. The two other eigenvalues can be influenced by varying K.

In figure 7 the root-locus is drawn for our reference gait $(\mathbf{x}^r, \mathbf{u}^r)$. As can be seen, the system can indeed be stabilized with the controller: by choosing a proper K, we can put both eigenvalues inside the unit circle. The system is stable for a reasonably large range of K. The minimum eigenvalue of -0.81 is reached when $K = 0.259$.

In order to see how well the controller with a fixed K can handle different limit cycles (different values for a and b in (8)), figure 8 was made. It shows that indeed a single value for K can stabilize a large region of limit cycles. We also see that the K that gave the lowest eigenvalues for our reference gait does really well in stabilizing faster gaits.

Eigenvalues only give insight in the behaviour under small disturbances. For a nonlinear system such as a walker, the behaviour under large disturbances is also very interesting. We are particularly interested in the *basin of attraction* [7]: how large can a disturbance be before the walker falls?

For investigation of the basin of attraction, it is useful to represent the velocity of the hip in polar coordinates v and β (see figure 9). A disturbance acting on β (affecting the direction of the velocity vector) will not affect the internal energy of the system, therefore the system can return to its original limit cycle. A disturbance acting on v (affecting the magnitude of the velocity vector) does affect the internal energy and will cause the walker to converge to a different limit cycle (if (v, β) is within the basin of attraction, that is). Note that in the limit cycle, b is small relative to a, which makes $v \approx a$.

Figure 10 shows a slice of the basin of attraction of the controlled system with $K = 0.259$. As can be seen, for low velocities the walker cannot be stabilized with this controller (there exists a limit cycle for these low velocities, but it is unstable). With increasing velocity the basin of attraction increases. From this we can conclude that fast walking more robust than slow walking. As most real walking robots have a relatively slow gait, this suggests that a bit of extra robustness could be obtained with relative ease by just making the robot walk faster.

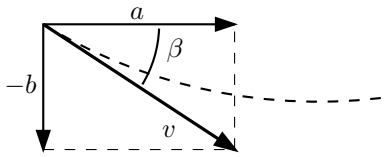

Fig. 9. Representation of the velocity of the hip as (v, β).

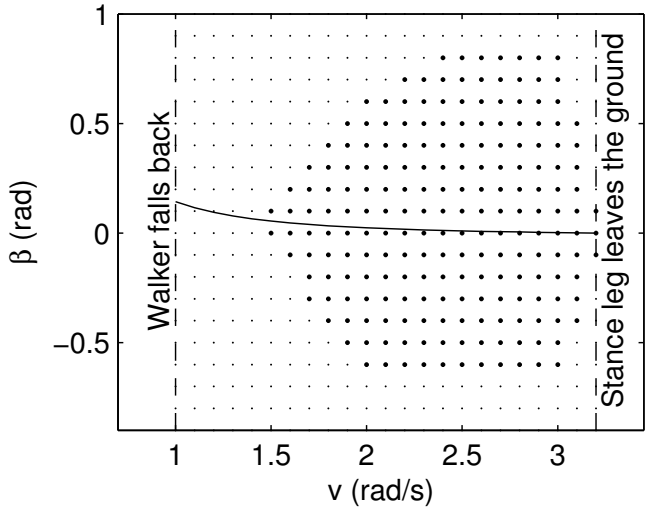

Fig. 10. The basin of attraction of the controlled system with controller gain $K = 0.259$. On the horizontal axis the velocity $v = \sqrt{a^2 + (-b)^2}$ is put, on the vertical axis we have $\beta = \text{atan}(\frac{-b}{a})$ (see also figure 9). Each dot represents a simulation run with initial condition $\mathbf{x}^+ = (\mathbf{u}_1^r, a, \mathbf{u}_2^r, -b)$. Large dots indicate that the initial condition is inside the basin of attraction. The curve in the graph shows the set of all limit cycles having $\mathbf{x}^* = (\mathbf{u}_1^r, \bullet, \mathbf{u}_2^r, \bullet)$. Note that for small velocities v the system is unstable and has no basin of attraction.

VII. Interpretation as a standard discrete nonlinear controller

When looking at the block diagram of the system (figure 5), it does not look like a standard discrete controller. However, $\mathcal{Y}_k$ is actually only dependent on $\mathbf{x}_k$ (via the equations of motion). So we can write: $\mathcal{Y}_k = f(\mathbf{x}_k)$ with f being a nonlinear function. This gives:

$$\mathbf{u}_k = \begin{pmatrix} \varphi_{hip,sw} \\ \varphi_{splay,sw} \end{pmatrix} = \begin{pmatrix} \mathbf{u}_1^* \\ \mathbf{u}_2^* + K \cdot f(\mathbf{x}_k) \end{pmatrix}$$

which is simply a conventional nonlinear controller. It is a special one however: because the value of $f(\mathbf{x}_k)$ has a clear geometrical meaning, this is much more insightful than just a nonlinear formula.

VIII. Conclusions and future work

A new method has been described for controlling lateral foot placement of a 3D compass biped model, based on time-reversal symmetry of the limit cycle. If a disturbance occurs, the step becomes asymmetric. It was shown that $\mathcal{Y} := \dot{\varphi}_{splay}|_{(\varphi_{hip}=0)}$ is a good measure for the degree of asymmetry of the step, and can be used for feedback. A proportional controller was proposed where the splay angle offset is proportional to $\mathcal{Y}$ (with controller gain K).

Simulation results showed that the controller can stabilize the walker in a large range of gaits (at different velocities) without any adjustment of the parameter, and that the basin of attraction is large, especially for fast walking. It was shown that the controller is actually a conventional nonlinear controller, with the additional property that the non-linear function has a clear geometrical meaning, which gives more insight in the actual control strategy.

The control method as described here works well with the compass model, but it cannot directly be used for more complex models, because generally the gait of such models is not time-reversal symmetric. This study will be continued by investigating how the method can be generalized to work with other walker models as well. Our goal is to build a real 3D biped soon, which will, amongst others, make use of the lateral foot placement control method.

Appendix
Proof that all limit cycles for a given $\mathbf{u}$ lie on one curve

It can be proven that there are infinitely many limit cycles for a given input $\mathbf{u}$. Let us first assume the movements in forward and sideways direction are uncoupled. For a normal step we can choose any forward velocity a as long as it is fast enough to push the walker over its highest point and slow enough to keep the foot on the ground, in spite of the centrifugal force. This a determines the step time $t_{step}(a)$, i.e. how long it takes to go from point $\mathbf{x}^+$ to $\mathbf{x}^-$. Because of the symmetry, it will take $t_{step}/2$ for the hip to reach $\varphi_{hip} = 0$. The sideways velocity $\mathcal{Y}$ at that moment can be calculated as follows:

$$\mathcal{Y} = \dot{\varphi}_{splay}|_{(\varphi_{hip}=0)} = -b + \int_0^{t_{step}(a)/2} \ddot{\varphi}_{splay}(\mathbf{x}(t))\,\mathrm{d}t$$

For each a there is exactly one $-b$ which leads to a limit cycle ($\mathcal{Y} = 0$). As infinitely many a's can be chosen (within the above described range), each with an associated $-b$, there are infinitely many limit cycles for a given $\mathbf{u}$, all lying on a one-dimensional curve segment.

References

[1] A. D. Kuo, "Stabilization of lateral motion in passive dynamic walking," *International Journal of Robotics Research*, vol. 18, no. 9, pp. 917–930, Sept. 1999.

[2] J. E. Pratt and G. A. Pratt, "Exploiting natural dynamics in the control of a 3D bipedal walking simulation," *Proceedings of the International Conference on Climbing and Walking Robots*, Sept. 1999.

[3] M. Wisse, "Essentials of dynamic walking," Ph.D. dissertation, TU Delft, Sept. 2004.

[4] V. Duindam, "Port-based modeling and control for effiecient bipedal walking robots," Ph.D. dissertation, University of Twente, 2006.

[5] S. H. Collins, M. Wisse, and A. Ruina, "A three-dimensional passive-dynamic walking robot with two legs and knees," *International Journal of Robotics Research*, vol. 20, no. 7, pp. 607–615, July 2001.

[6] G. van Oort, "Strategies for stabilizing a 3D dynamically walking robot," Master's thesis, University of Twente, June 2005.

[7] A. Schwab and M. Wisse, "Basin of attraction of the simplest walking model," *ASME 2001 Design Engineering Technical Conferences*, vol. DETC2001/VIB-21363, Sept. 2001.